Int. J. Multiphase Flow Vol. 14, No. 6, pp. 749–763, 1988
Printed in Great Britain.

0301-9322/88 $3.00 + 0.00

WAKE PROPERTIES OF A SINGLE GAS BUBBLE IN A THREE-DIMENSIONAL LIQUID–SOLID FLUIDIZED BED

T. MIYAHARA, K. TSUCHIYA and L.-S. FAN†
Department of Chemical Engineering, The Ohio State University, Columbus, OH 43210, U.S.A.

(*Received* 25 *December* 1987; *in revised form* 18 *June* 1988)

Abstract—Experiments were performed to investigate the wake properties of a single gas bubble in a three-dimensional liquid–solid fluidized bed via a video camera moving at the same speed as the bubble. The solids holdup in the fluidized bed varied up to around 10%. The bubble size varied from 5 to 20 mm with corresponding bubble Reynolds numbers ranging from 1000 to 6500. The bubble was observed to have two types of wake configurations depending on the bubble size: the asymmetric/helical vortex wake for small bubbles and the symmetric wake for large bubbles. The bubble shape and relative rise velocity in the fluidized bed can be well-represented by correlations developed for single bubbles in liquid media, although the bubble shape in liquid–solid media is slightly more flattened compared to that in liquid media. The bubble rocking frequency was found to be independent of particle properties and to correspond in magnitude to the vortex shedding frequency in a two-dimensional liquid–solid fluidized bed. The average primary wake size in three dimensions is comparable to that in two dimensions.

Key Words: bubble wake, liquid–solid, fluidized bed, helical vortex, symmetric wake, bubble rocking, vortex shedding

INTRODUCTION

In a gas–liquid–solid fluidized bed, solid particles are fluidized by the liquid and/or gas flows, giving intimate mixing of individual phases. The three-phase fluidized bed has been used in such processes as polymerization, resid hydrotreating and biological waste water treatment. Prior interest in fundamental three-phase fluidization research has been primarily on the transport properties of the systems, i.e. the phase holdups and heat and mass transfer behavior. Very little information, however, is available regarding fluid mechanic behavior associated with the bubble wake, which plays a dominant role in dictating the transport properties of the system, particularly the solids mixing.

In three-phase fluidization, the bubble wake is defined as the liquid–solid region immediately behind the bubble traveling at the same velocity as that of the bubble. Darton & Harrison (1976) theoretically predicted the height of the liquid wake based on steady wake configurations and gave a reasonable quantitative estimation of the liquid wake size for large spherical-cap bubbles. Rigby & Capes (1970) made a direct measurement of the liquid wake size of a single bubble rising in a two-dimensional liquid–solid fluidized bed. Rigby & Capes also pointed out the non-negligible contribution of shed vortices, which characterize the dynamic nature of the bubble wake, to the bed contraction phenomenon. In light of these important studies, Tsuchiya & Fan (1986) recently investigated, from the fluid mechanic point of view, the near-wake structure of a relatively large single gas bubble in a two-dimensional liquid–solid fluidized bed. They identified and defined the primary wake, which is fluid mechanically distinct from the far wake in the sense that it is responsible for the vortex formation but is relatively insensitive to external flow conditions.

The three-dimensional structures of the bubble wake, however, have not been studied in gas–liquid–solid fluidized beds. Although some studies have been conducted in gas–liquid systems (e.g. Maxworthy 1967; Slaughter & Wraith 1968; Lindt 1972; Wegener & Parlange 1973; Lindt & de Groot 1974; Narayanan *et al.* 1974; Kojima *et al.* 1975; Coppus *et al.* 1977; Yabe & Kunii 1978; Komasawa *et al.* 1980; Bhaga & Weber 1981; Bessler 1984), detailed structures are still not fully understood at large bubble Reynolds numbers. In general, for large spherical-cap bubbles at Re

†To whom correspondence should be addressed.

(defined based on the equivalent spherical diameter of the bubble, d) <100–110 (Wegener & Parlange 1973; Bhaga & Weber 1981) the bubble wake is considered to be laminar. The primary wake is closed and clearly defined by a stationary toroidal vortex ring, or a deformed Hill's vortex. The wake is stable and sheds no vortex. When the Re exceeds a critical value, the vortices formed in the primary wake are no longer stationary but are discharged from the bubble. The periodicity of vortex shedding behind the bubble has been confirmed in both two-dimensional (Rigby & Capes 1970; Lindt 1971; Tsuchiya & Fan 1986) and three-dimensional systems (Lindt 1972; Lindt & de Groot 1974); however, the structure of the bubble wake is still far from comprehension, particularly in three dimensions.

The wake structures behind a fixed bluff object in a uniform fluid flow have been studied to some extent. Although not definite, as in the case of gas bubbles, the following wake configurations have been observed or at least speculated: (1) a helical/spiral vortex; (2) bi-spiral vortices; (3) toroidal vortices; and (4) a sequence of irregularly shaped vortex loops whose shape may be characterized by horseshoes. Levy & Forsdyke (1927, 1928) and Jeffreys (1930) found that the helical vortex, bi-spiral vortices or toroidal vortices wake was theoretically unstable. The horseshoe vortex loops were theoretically speculated by Rosenhead (1953) and visually observed by Achenbach (1974) for fixed solid spheres at $Re = 400$ to 3000. For bubbles ranging from intermediate size (oblate spheroidal) to large size (spherical-cap), Lindt (1972) and Lindt & de Groot (1974) observed a helical vortex indirectly from the associated bubble motion and directly from flow visualization (a two-dimensional view of the wake flow) for a Reynolds number (based on the bubble major axis, a), Re′, of 1800–6200 and 90–620, respectively. Yabe & Kunii (1978) observed the horseshoe vortex loops discharged behind a large spherical-cap bubble at $Re = 70$ to 250.

The present study extends the two-dimensional study conducted by Tsuchiya & Fan (1986) to a three-dimensional system. The dynamic nature of the bubble wake is visualized via a video camera rising at the same speed as the bubble. Besides the wake properties, the shape and rise velocity of relatively large single bubbles are presented. Comparisons are made of the bubble wake behavior between two- and three-dimensional liquid–solid fluidized beds.

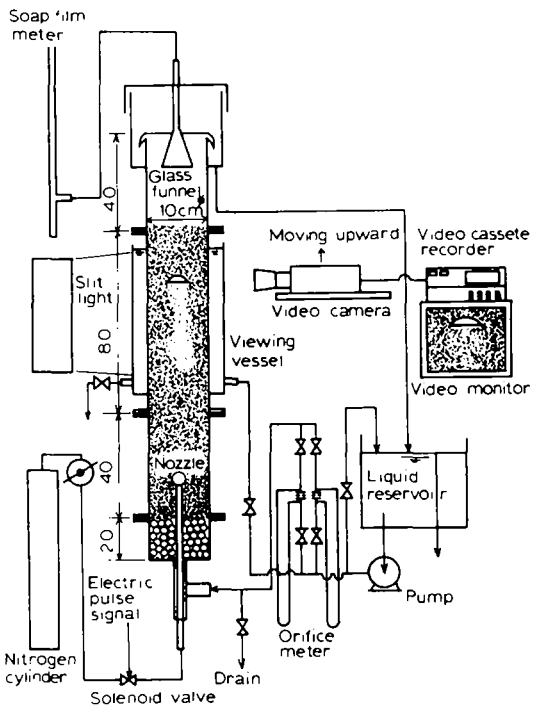

Figure 1. Schematic diagram of the experimental apparatus (in cm).

Table 1. Physical properties of spherical particles

	Average dia (mm)	Density (kg/m^3)	Terminal velocity (10^{-2}m/s)	Material	Solids holdup (%)
GB460	0.46	2500	7.46	Glass	6.3
AT1000	1.0	1252	4.94	Acetate	4.5
AR1500	1.5	1183	5.98	Polymethyl methacrylate	8.3
SR2000	2.0	1050	3.36	Polystyrene	10.1

EXPERIMENTAL

The experimental apparatus for the three-dimensional system is shown schematically in figure 1. The Plexiglas column is of 0.1 m i.d. and the test section is 0.8 m high. The column i.d. is considered to be large enough to yield negligible wall effects on the shape and rise velocity of a bubble of equivalent diameter up to 20 mm (Uno & Kintner 1956; Calderbank 1967). Upon injection, the bubble rapidly accelerated and attained terminal velocity in a distance <0.4 m. The test section is enclosed in a rectangular viewing vessel made of Plexiglas and filled with tap water to minimize optical distortion. A uniform liquid distribution was achieved using a fixed bed containing glass beads of 6 mm dia supported on 20-mesh wire cloth. A single gas bubble was generated from a nozzle of 3.5 mm i.d. at the center of the column bottom using a solenoid valve connected to a micro-switch. The location of the micro-switch was arranged so that the bubble injection timing could be synchronized with the timing of the video camera (Panasonic WV-1800) rise. The bubble size was varied by altering the gas delivery pressure and the opening time of the solenoid valve. The details of the vertical camera transport system are described in Tsuchiya & Fan (1986).

Lighting was applied from the side through a slit to provide a narrow vertical light sheet along the vertical distance traveled by a bubble to obtain a two-dimensional view of the wake flow. The data were recorded by a video recorder. In the preliminary runs the bubble volume was determined based on two methods: (1) a direct measurement using a soap film flow meter; and (2) a calculation based on the assumption of an ellipsoidal shape using bubble dimensions measured in two-dimensional projection. The two methods agreed within $\pm 10\%$ deviation. The second method was used to determine the bubble size in this study.

Tap water and nitrogen were employed, respectively, as the liquid and gas phases. The superficial liquid velocity varied from 0.02 to 0.06 m/s. The physical properties of four different types of spherical particles used in this study are listed in table 1. Note that the ratio of bubble to particle size ranged from 5 to 37. The solids holdup range under study was limited to about 10% due to clarity constraints in the visualization technique. The Richardson–Zaki equation (Richardson & Zaki 1954) given below for the relationship between the superficial liquid velocity, U_L, and liquid holdup, ϵ_L, was applied to determine the solids holdup in the liquid–solid fluidized bed:

$$U_L = U_T \epsilon_L^n \qquad [1]$$

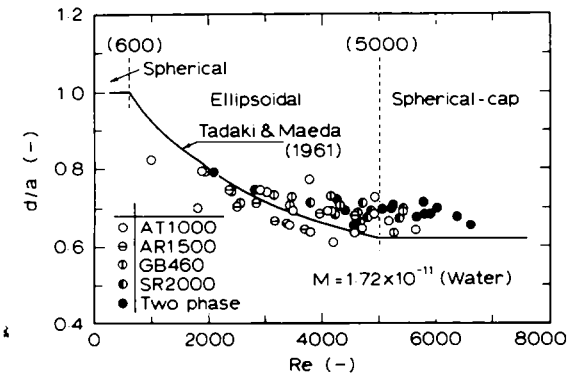

Figure 2. Bubble shape in the liquid–solid fluidized bed.

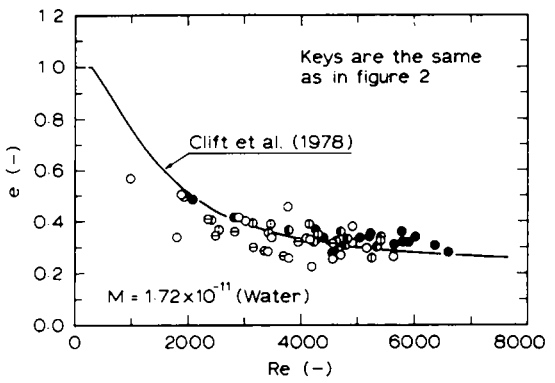

Figure 3. Bubble aspect ratio in the liquid–solid fluidized bed.

where U_T is the particle terminal velocity and n, the Richardson–Zaki index, can be expressed (Garside & Al-Dibouni 1977) by

$$n = \frac{5.1 + 0.28\,\mathrm{Re}_p^{0.9}}{1.0 + 0.1\,\mathrm{Re}_p^{0.9}},\quad \mathrm{Re}_p = \frac{d_p U_T \rho_L}{\mu_L},$$

where Re_p is the particle Reynolds number, d_p is the particle diameter and ρ_L and μ_L are the density and viscosity of the liquid, respectively. For reference, experiments were also carried out for a gas-liquid system with plyolite particles ($\rho_s = 1024\,\mathrm{kg/m^3}$, $d_p = 250$–$380\,\mu\mathrm{m}$) as the liquid flow tracer.

RESULTS AND DISSCUSION

Bubble Rise Characteristics

It is known that the rise characteristics of bubbles in liquid and/or liquid–solid media, such as the shape, rise velocity and oscillations of bubbles, are closely related to the bubble wake behavior. In the following, such bubble rise characteristics in the liquid–solid fluidized media are discussed and compared with those in a stationary liquid.

Bubble shape

The bubble shape in stationary liquids is usually classified by spherical, ellipsoidal and spherical-cap bubbles. Tadaki & Maeda (1961), based on a large number of data on bubble shapes

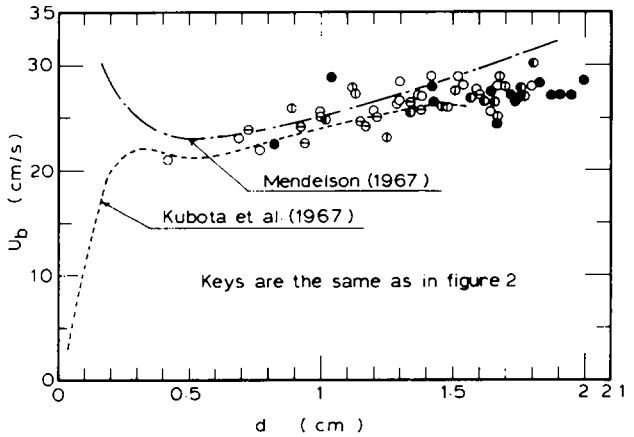

Figure 4. Bubble rise velocity in the liquid-solid fluidized bed.

in various liquids over a wide range of the bubble Reynolds number, Re, presented the following empirical correlations for the bubble deformation factor, d/a:

$$d/a = 1, \qquad \mathrm{ReM}^{0.23} < 2 \text{ (spherical)}, \qquad [2]$$

$$d/a = 1.14(\mathrm{ReM}^{0.23})^{-0.176}, \qquad 2 \leqslant \mathrm{ReM}^{0.23} < 6 \qquad [3]$$

$$d/a = 1.36(\mathrm{ReM}^{0.23})^{-0.28}, \qquad 6 \leqslant \mathrm{ReM}^{0.23} < 16.5 \qquad [4]$$

(ellipsoidal),

$$d/a = 0.62, \qquad 16.5 \leqslant \mathrm{ReM}^{0.23} \text{ (spherical-cap)}, \qquad [5]$$

where the rise velocity in Re is defined based on the bubble velocity relative to the surrounding liquid, U_b, and M ($=g\mu_L^4/\rho_L\sigma^3$) is the Morton number. Here g denotes the acceleration due to gravity and σ the surface tension. Figure 2 gives the bubble deformation factor as a function of Re. The figure includes the present data for liquid and liquid–solid fluidized beds involving four types of particles and the Tadaki & Maeda (1961) correlations ([2]–[5]). As can be seen in the figure, the bubble shape in the liquid–solid fluidized beds can be well-represented by the Tadaki & Maeda correlations.

The difference in the bubble shape is more pronounced when a plot of the bubble aspect ratio (minor axis/major axis), e, is made against Re, as given in figure 3. The solid line in figure 3 is an extension of the Tadaki & Maeda correlations for single bubbles in liquids (Clift *et al.* 1978) as expressed by

$$e = 1, \qquad \mathrm{ReM}^{0.23} < 1, \qquad [6]$$

$$e = [0.81 + 0.206 \tanh\{2(0.8 - \log_{10} \mathrm{ReM}^{0.23})\}]^3, \qquad 1 \leqslant \mathrm{ReM}^{0.23} < 39.8, \qquad [7]$$

$$e = 0.24, \qquad 39.8 \leqslant \mathrm{ReM}^{0.23}. \qquad [8]$$

It is clearly seen in the figure that the bubble shape in the liquid–solid fluidized beds tends to be more flattened, as reflected by a smaller e, than that in liquid alone at the same Re; however, no systematic variation with respect to the particle properties was seen.

Bubble rise velocity and drag coefficient

Figure 4 shows the variation of the bubble rise velocity relative to the surrounding liquid with the equivalent spherical diameter of the bubble. It can be seen from the figure that the bubble rise velocity in the present systems is comparable in magnitude with that in liquids reported by Kubota *et al.* (1967). The figure also shows the theoretical rise velocity of relatively large bubbles in stationary liquids predicted by the wave theory (Mendelson 1967) as

$$U_b = \sqrt{\frac{2\sigma}{d\rho_L} + \frac{gd}{2}}. \qquad [9]$$

This equation, which neglects viscous effects, gives a reasonable estimation of the bubble rise velocity in both water and water–solid fluidized media with a low solids holdup for bubble size $d > 5$ mm. The present results indicate that the presence of particles at low solids holdup ($< 10\%$) has no appreciable effects on the bubble rise velocity.

The terminal rise velocity of the bubble is reached when the net buoyancy force balances the drag force acting on the bubble. The drag force acting on the bubble can be represented by the drag coefficient. Considering the bubble shape, the drag coefficient, C'_D, can be expressed by (Takahashi *et al.* 1976)

$$C'_D = \left(\frac{d}{a}\right)^2 \frac{4gd}{3U_b^2} = \left(\frac{d}{a}\right)^2 C_D, \qquad [10]$$

where C_D is the drag coefficient evaluated based on a bubble with an equivalent spherical diameter. Figure 5 shows the drag coefficient calculated based on [10] and the experimental data over a wide Reynolds number range. As seen in the figure, the drag coefficients of single bubbles in the liquid and liquid–solid systems are nearly constant over the entire Reynolds number range considered and have average values of 1.13 and 1.45, respectively, for the gas–liquid and gas–liquid–solid systems. Note that in figure 5 other systems are also indicated, including solid spheres in fluids, bubble

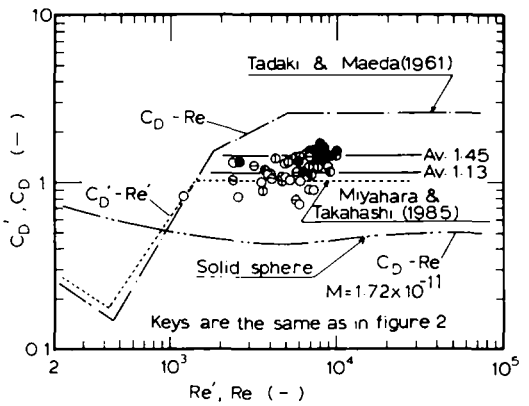

Figure 5. Drag coefficient of single bubbles in the liquid solid fluidized bed.

spheres (equivalent) in water (Tadaki & Maeda 1961) and deformed bubbles in water (Miyahara & Takahashi 1985).

Bubble gyration/rocking angle

In the bubble size range considered, bubbles rise with some oscillations in path. Figure 6 shows the degree of oscillation (or lateral displacement) in terms of the bubble inclined angle, θ, defined in the figure. The figure shows that θ is almost independent of Re with an average value of 25° for Re up to about 5000. It, however, abruptly decreases with Re when Re > 5000. Note that this demarcation Re (Re = 5000) also marks the transition from an ellipsoidal to spherical-cap bubble shape, as shown in figure 2.

The mode of oscillation for small bubbles (Re < 5000) was a gyrational motion, which corresponds to rocking in two dimensions. Note, however, the bubble itself was not observed to revolve about its center axis. A vertically rising bubble thus followed a helix-like path. As the bubble size increased (Re > 5000), bubble gyration became almost negligible (i.e. with very small θ) and the bubble rose almost rectilinearly.

Bubble Wake Structure

Figures 7 and 8 show photographs and a schematic interpretation of gyrating bubbles (Re ⩽ 5000) and their wakes in stationary water and in a water–1 mm acetate particle fluidized bed, respectively. As can be seen in both figures, the structure of the wake can be represented by an asymmetric wake about the vertical axis of the bubble movement. Bubbles in this regime usually experience significant shape oscillations, which in general occur in a random manner. This shape asymmetry and rather periodic variation in the bubble orientation may yield non-uniform flow

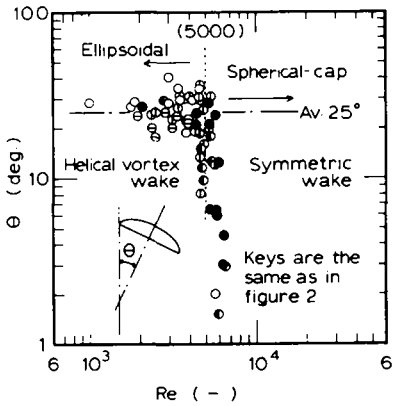

Figure 6. Bubble inclined angle in the liquid–solid fluidized bed.

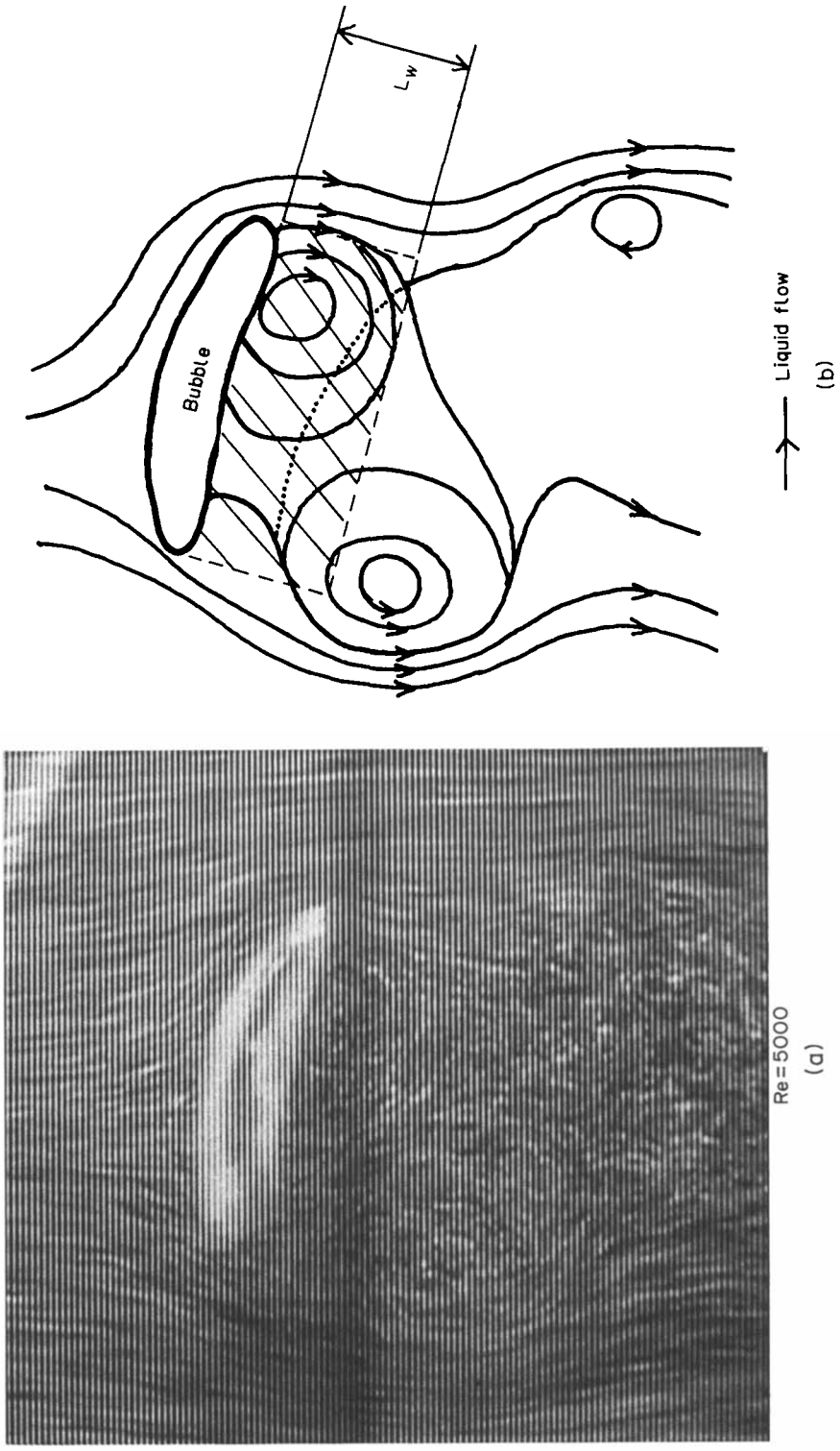

Figure 7. (a) Photograph of a bubble rising through stationary water and its wake (helical vortex wake). (b) Schematic drawing of the wake.

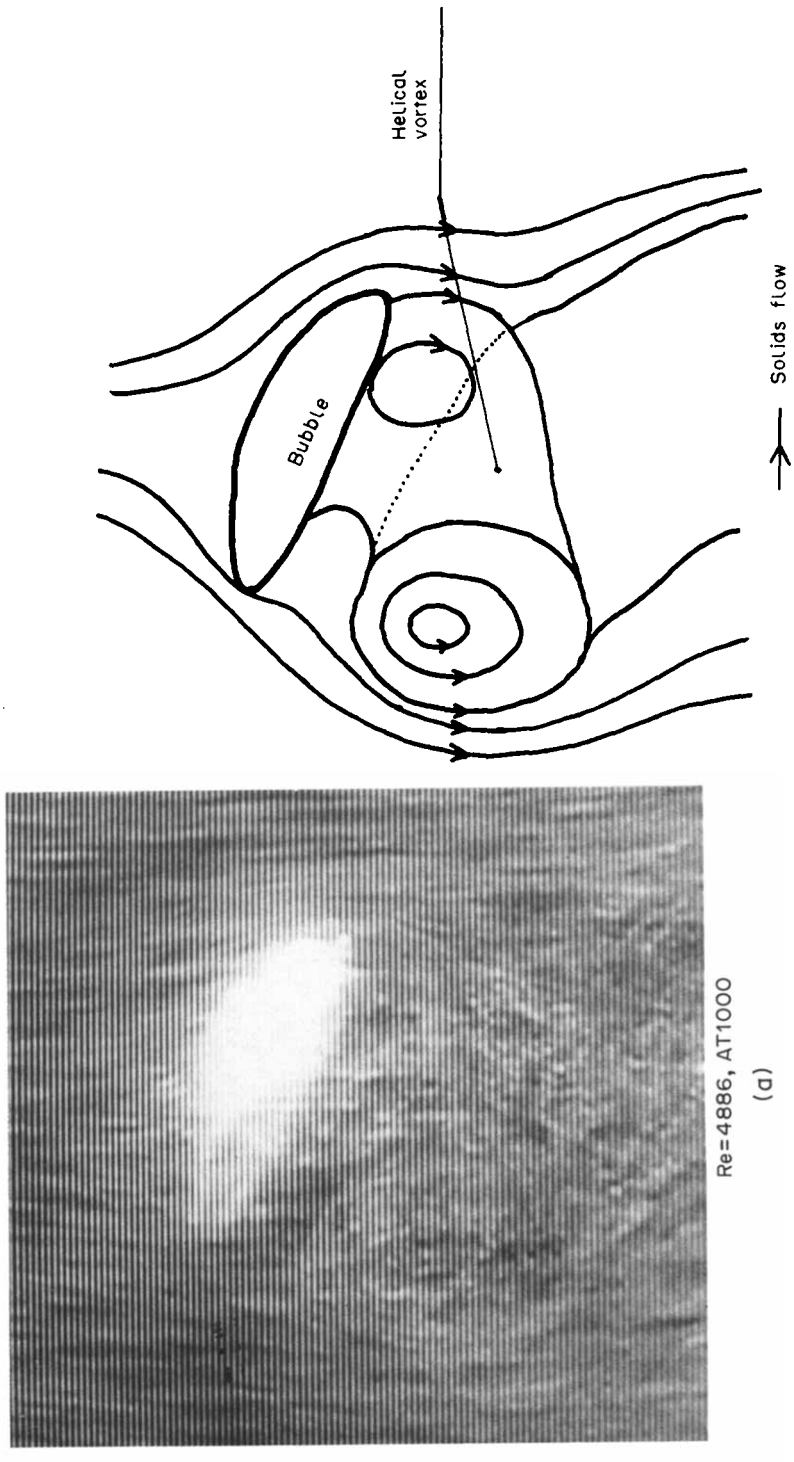

Figure 8. (a) Photograph of a bubble rising through a water 1 mm acetate particle fluidized bed and its wake (helical vortex wake). (b) Schematic drawing of the wake.

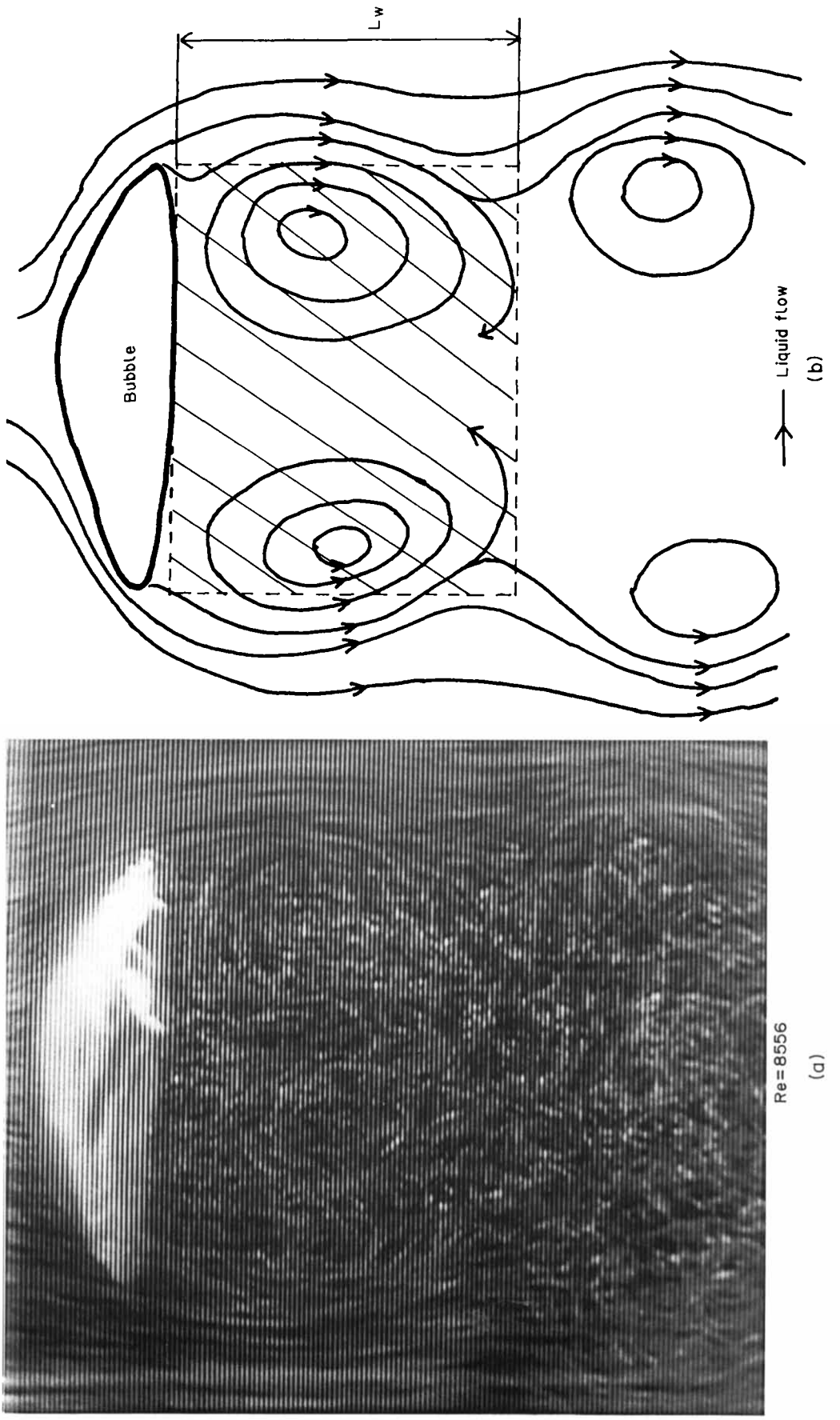

Figure 9. (a) Photograph of a bubble rising through stationary water and its wake (symmetric wake). (b) Schematic drawing of the wake.

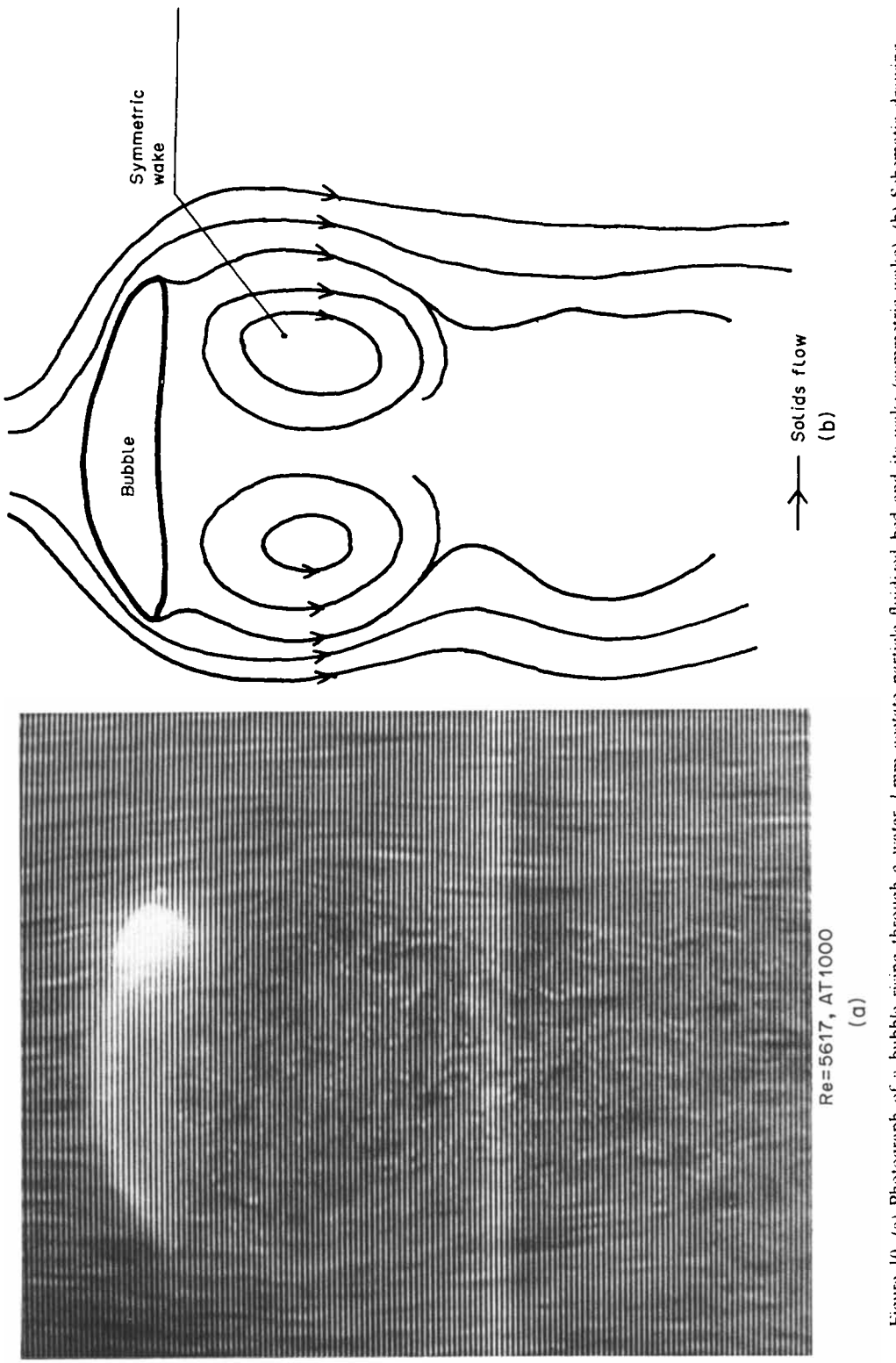

Figure 10. (a) Photograph of a bubble rising through a water–1 mm acetate particle fluidized bed and its wake (symmetric wake). (b) Schematic drawing of the wake.

separation along the bubble edge. The biased flow separation then induces locally-strong vorticity generation, which eventually forms a vortex filament constantly discharged from the portion of the bubble edge with the "biased" flow separation. Observation of dynamic motion of the separation region from the VTR revealed that this "strong" separation region actually rotates around the bubble edge. The frequency of this rotation was found to match the bubble gyration frequency.

It is worth noting that the rotating separation process is supported by an important finding reported by Achenbach (1974). Achenbach conducted hot-wire measurements of velocity fluctuations around the surface of a stationary solid sphere in a wind tunnel. The hot-wire signals recorded simultaneously at different positions on a periphery near the separation region in the Re range $6 \times 10^3 < \mathrm{Re} < 3 \times 10^5$ showed a phase shift. Achenbach interpreted this finding as that "the vortex separation occurs at a point and that the point of vortex release rotates around the sphere with the vortex shedding frequency". Note that this "point-wise vortex separation" can be more pronounced for a freely rising, deformed bubble than for a rigidly supported sphere.

Based on the above experimental evidence and discussion, a physical illustration of the wake structure behind an intermediate-size bubble may be in order. The separation of the boundary layer formed along the bubble frontal surface takes place at a point along the bubble rim. The vorticity generated at the separation point is discharged downstream in the form of a vortex filament. This vortex filament tends to move towards the wake center axis due to the pressure defect in the wake region and at the same time to form a spiral due to the rotation of the separation point along the bubble rim. The resulting wake structure is the continuous discharge of a vortex filament spiraling about the wake center axis whose pitch is controlled by the bubble gyration frequency and the downward vortex-discharging velocity. The intermittent appearance of a vortex pair on the plane of visualization at a constant frequency, which corresponds to the bubble gyration frequency, was observed in the experiment: this observation is strong evidence for the above illustration. The presence of a helical vortex is also supported by Lindt (1972) and Lindt & de Groot (1974) for ellipsoidal and spherical-cap bubbles of intermediate sizes.

Figures 9 and 10 show photographs and sketches of the bubble wake structure and flow field surrounding the bubble in stationary water and in a water–1 mm acetate particle fluidized bed, respectively. The Re for the figures is >5000. As can be seen in both figures, the structure of the wake can be represented by a symmetric wake about the vertical axis of the bubble movement. As the bubble Re increases beyond 5000, the bubble tends to discharge vorticity symmetrically in the form of either a set of apparently discontinuous toroidal vortices (or vortex rings) or two continuous helical vortices (or bi-spiral vortices). The present visualization study cannot distinguish these two configurations due to the limitation in clarity.

It should be noted that the projected views of the near-wake structures of the three-dimensional bubble wake shown in figures 7–10 are very similar to the near-wake structures of the bubbles in the two-dimensional system observed by Tsuchiya & Fan (1986). Tsuchiya & Fan (1986) identified alternate vortex shedding for intermediate-size bubbles which resembles the projected view of the helical vortex shedding (figures 7 and 8). They also identified parallel vortex shedding for large-size bubbles which resembles the projected view of the symmetric vortex shedding (figures 9 and 10).

Bubble Rocking/Wake Shedding Frequency

The wake shedding frequency in the present study was determined based on the time for the bubble to complete one rocking cycle. Figure 11 shows the Strouhal number, St ($=af_c/U_b$), as a function of the Re′ based on the bubble major axis in both gas–liquid and gas–liquid–solid systems. Here f_c is the bubble rocking or wake shedding frequency. The figure also includes the results of Lindt (1972) for an air–tap water system. It is seen that there is no systematic variation of the St due to differences in particle properties or even the presence/absence of particles, nor with the difference in wake shedding modes, including helical vortex and symmetric wake shedding modes. The St increases monotonically with increasing Re′. Similar trends were observed for bubbles in a two-dimensional stationary water or liquid–solid fluidized bed (Rigby & Capes 1970; Lindt 1971; Tsuchiya & Fan 1986). Note that the solid line in the figure corresponds to the alternate shedding frequency of vortex pairs in the two-dimensional fluidized bed correlated by Tsuchiya & Fan (1986). The wake shedding frequencies in both two- and three-dimensional systems fall within the same range. This fact reflects that the findings obtained in a two-dimensional system may be

applicable to a three-dimensional system. Also, based on the current experimental results, the following empirical correlation can be obtained:

$$\mathrm{St} = 0.0013\,\mathrm{Re}'^{2/3}, \qquad 10^3 < \mathrm{Re}' < 10^4. \qquad [11]$$

Wake Size

Tsuchiya & Fan (1986) defined the primary wake boundary in two dimensions by the cut-off stream crossing the wake center axis from one side of the wake to the other or, if the cut-off stream is difficult to identify, by the line connecting the outermost streamlines of the vortices at each side of the wake. The above definition could apply to three-dimensional systems, although determination of the cut-off stream on the plane of visualization is not straightforward due to its intermittent appearance. Thus, the primary wake size in three dimensions was estimated based on the distance from the bubble base to the base of the primary vortex appearing on the plane of visualization, L_w, schematically defined in figures 7 and 9.

The first measure of the wake size is the primary wake length normalized with respect to the bubble major axis. Figure 12 shows the average value of several instantaneous ratios (L_w/a) measured for each bubble over the Re′ range considered in the present study. No drastic time variation of the wake size was observed in each cycle of the wake shedding process as occurred in a two-dimensional system (Tsuchiya & Fan 1986); thus only the average values are reported here. The dimensionless wake length values lie scattered around averages of 0.6 and 1 for the helical vortex and symmetric wakes, respectively, and exhibit no systematic variation with respect to the Re′ or particle properties.

Figure 13 shows the variation of the ratio of the wake volume, V_w, to the bubble volume, V_b, with the Re′. The wake volume was defined according to Kojima *et al.* (1975) as

$$V_w = \frac{\pi}{4} a^2 L_w. \qquad [12]$$

The wake-to-bubble volume ratio is independent of the Re′ and has a mean value of 2.5 for the helical vortex wake and around 4.7 for the symmetric wake. The latter is the same value as that found by Kojima *et al.* (1975) for spherical-cap bubbles in a liquid ($2000 < \mathrm{Re} < 5000$). The figure also includes the results of Coppus *et al.* (1977) and Komasawa *et al.* (1980) who reported the values of 22 and 26, respectively, which are much greater than the present results. This discrepancy may be attributed to the fact that Coppus *et al.* (1977) and Komasawa *et al.* (1980) obtained the wake volume of very large spherical-cap bubbles (up to 8 cm in breadth) mostly in high-viscosity liquids; the liquid viscosities were as high as 130 and 712 cP, respectively. It is known that high viscosity stabilizes the wake (Bhaga & Weber 1981). It is noted that the values of the wake-to-bubble volume ratio obtained for single bubbles in two-dimensional liquid–solid fluidized beds were of the same order of magnitude: Henriksen & Ostergaard (1974) reported the normalized wake height to be about 1.2 and Tsuchiya & Fan (1986) reported the volume ratio to be 4.2.

Estimation of Bubble Rise Path

Based on the aforementioned bubble rise behavior the bubble rise path can be estimated. Figure 14 shows the observed bubble movement expressed in terms of the bubble locations at different times. Here only locations A and B give the "true projected shape" in a two-dimensional view. At location A the bubble center, defined as the midpoint of the bubble major axis and designated by C in the figure, can be specified. Note that the bubble center C rises a distance $U_b/4f_c$ in the vertical direction during one-quarter of a bubble rocking cycle and has a maximum lateral displacement from the vertical axis of the bubble movement, $U_b \tan\theta/4f_c$, at location A. In the calculation $\theta = 25°$ was utilized (see figure 6). Now theoretical locations of the centers E and F can be specified. The same procedure can be applied to obtain point G at one-half cycle and H at one cycle. Since the path line EFG of the bubble center is a helix, the estimated bubble rise path can be expressed in the following mathematical form:

$$x^2 + y^2 = \left(\frac{U_b}{4f_c}\tan\theta\right)^2, \; y = x\tan\left(\frac{2\pi f_c z}{U_b}\right), \qquad [13]$$

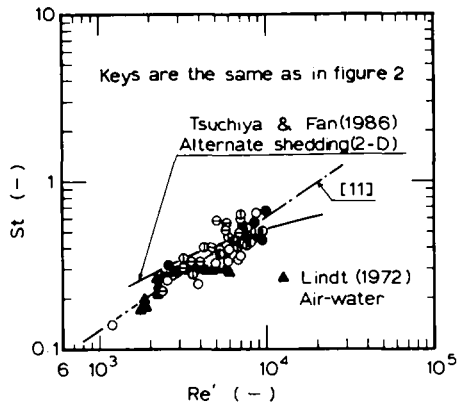

Figure 11. St as a function of the Re′ (based on the bubble major axis).

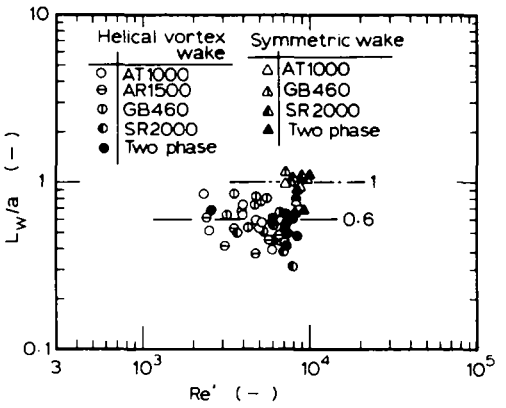

Figure 12. Wake height in the liquid-solid fluidized bed.

where x and y represent the horizontal positions and z the vertical. The estimated locus of the bubble center is given by the dashed curve in figure 14. Reasonable agreement is found between this curve and the observed bubble rise path.

CONCLUDING REMARKS

Over the bubble size range investigated in this study ($5 < d < 20$ mm), the bubble in a three-dimensional liquid–solid fluidized bed rises in one of two different patterns: (1) with spiraling at an almost constant inclined angle of 25° without rotation; and (2) in a rectilinear path. The former is characteristic of small-size bubbles and the latter of large bubbles. The transition takes place rather sharply at Re ≈ 5000, which also corresponds to the bubble shape transition from an ellipsoid to spherical-cap. The bubble shape and relative rise velocity in the liquid–solid fluidized bed of low solids holdup can be predicted by existing correlations for liquid alone, although the bubble shape in the liquid–solid system is slightly more flattened than that in liquid.

Two types of wake configurations were observed: (1) a helical vortex wake and (2) a symmetric wake. The helical vortex, which is intimately related to the spiral rise of intermediate-size bubbles, is a result of "point-wise" flow separation rotating around the bubble edge. The frequency of the rotation synchronizes with that of bubble rocking. The symmetric wake, which is discharged when the bubble inclined angle approaches zero with increasing bubble size, may result from uniform flow separation along the bubble rim.

The St number increases monotonically with the bubble Re′ but is independent of particle properties and wake shedding mode. The St–Re′ relationship in three dimensions can be predicted

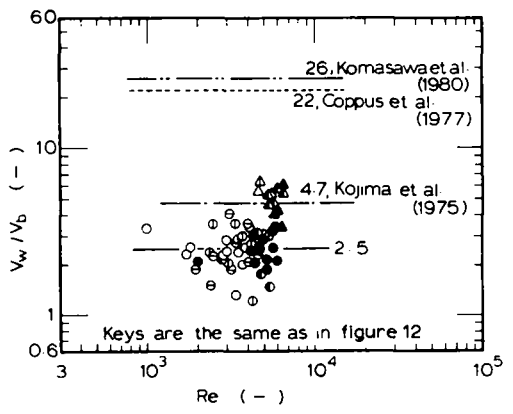

Figure 13. Wake volume in the liquid–solid fluidized bed.

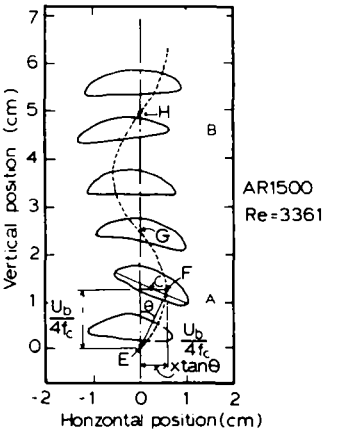

Figure 14. Two-dimensional projection of a bubble rise path.

from that in two dimensions. The mean wake volume in three dimensions is estimated to be 2.5 times the bubble volume for the helical vortex wake and 4.7 for the symmetric wake. The measured bubble and wake properties were used to theoretically predict the bubble rise path based on the helical vortex concept.

Acknowledgements—This work was sponsored by National Science Foundation Grant CBT-8516874.

REFERENCES

ACHENBACH, E. 1974 Vortex shedding from spheres. *J. Fluid Mech.* **62,** 209–221.

BESSLER, W. F. 1984 Analytical and experimental studies of wakes behind circularly capped bubbles. Ph.D. Dissertation, R.P.I., New York.

BHAGA, D. & WEBER, M. E. 1981 Bubbles in viscous liquids: shapes, wakes and velocities. *J. Fluid Mech.* **105,** 61–85.

CALDERBANK, P. H. 1967 Review series No. 3 gas absorption from bubbles. *Trans. Instn chem. Engrs* **45,** CE209–CE233.

CLIFT, R., GRACE, J. R. & WEBER, M. E. 1978 *Bubbles, Drops, and Particles.* Academic Press, New York.

COPPUS, J. H. C., RIETEMA, K. & OTTENGRAF, S. P. P. 1977 Wake phenomena behind spherical-cap bubbles and solid spherical-cap bodies. *Trans. Instn chem. Engrs* **55,** 122–129.

DARTON, R. C. & HARRISON, D. 1976 Bubble wake structure in three-phase fluidization. In *Fluidization Technology*, Vol. I (Edited by KEAIRNS, D. L.), pp. 399–403. Hemisphere, Washington, D.C.

GARSIDE, J. & AL-DIBOUNI, M. R. 1977 Velocity–voidage relationships for fluidization and sedimentation in solid–liquid systems. *Ind. Engng Chem. Process Des. Dev.* **16,** 206–214.

HENRIKSEN, H. K. & OSTERGAARD, K. 1974 Characteristics of large two-dimensional air bubbles in liquids and in three-phase fluidized beds. *Chem. Engng J.* **7,** 141–146.

JEFFREYS, H. 1930 The wake in fluid flow past a solid. *Proc. R. Soc. Lond. A* **128,** 376–393.

KOJIMA, E., AKEHATA, T. & SHIRAI, T. 1975 Behavior of single air bubbles held stationary in downward flow. *J. chem. Engng Japan* **8,** 108–113.

KOMASAWA, I., OTAKE, T. & KAMOJIMA, M. 1980 Wake behavior and its effect on interaction between spherical-cap bubbles. *J. chem. Engng Japan* **13,** 103–109.

KUBOTA, M., AKEHATA, T. & SHIRAI, T. 1967 Behavior of single air bubbles in low-viscosity liquids. *Kagaku Kogaku* **31,** 1074–1080.

LEVY, H. & FORSDYKE, G. 1927 The stability of an infinite system of circular vortices. *Proc. R. Soc. Lond. A* **114,** 594–604.

LEVY, H. & FORSDYKE, G. 1928 The steady motion and stability of a helical vortex. *Proc. R. Soc. Lond. A* **120,** 670–690.

LINDT, J. T. 1971 Note on the wake behind a two-dimensional bubble. *Chem. Engng Sci.* **26,** 1776–1777.

LINDT, J. T. 1972 On the periodic nature of the drag on a rising bubble. *Chem. Engng Sci.* **27,** 1775–1781.

LINDT, J. T. & DE GROOT, R. G. F. 1974 The drag on a single bubble accompanied by a periodic wake. *Chem. Engng Sci.* **29,** 957–962.

MAXWORTHY, T. 1967 A note on the existence of wakes behind large, rising bubbles. *J. Fluid Mech.* **27,** 367–368.

MENDELSON, H. D. 1967 The prediction of bubble terminal velocities from wave theory. *AIChE Jl* **13,** 250–253.

MIYAHARA, T. & TAKAHASHI, T. 1985 Drag coefficient of a single bubble rising through a quiescent liquid. *Int. chem. Engng* **25,** 146–148.

NARAYANAN, S., GOOSSENS, L. H. J. & KOSSEN, N. W. F. 1974 Coalescence of two bubbles rising in line at low Reynolds numbers. *Chem. Engng Sci.* **29,** 2071–2082.

RICHARDSON, J. F. & ZAKI, W. N. 1954 Sedimentation and fluidization: part I. *Trans. Instn chem. Engrs* **32,** 35–53.

RIGBY, G. R. & CAPES, C. E. 1970 Bed expansion and bubble wakes in three-phase fluidization. *Can. J. chem. Engng* **48,** 343–348.

ROSENHEAD, L. 1953 Vortex systems in wakes. In *Advances in Applied Mechanics*, Vol. III Edited by VON MISES, R. & VON KARMAN, T.), pp. 185–195. Academic Press, New York.

SLAUGHTER, I. & WRAITH, A. E. 1968 The wake of a large gas bubble. *Chem. Engng Sci.* **23,** 932.

TADAKI, T. & MAEDA, S. 1961 On the shape and velocity of single air bubbles rising in various liquids. *Kagaku Kogaku* **25,** 254–264.

TAKAHASHI, T., MIYAHARA, T. & IZAWA, H. 1976 Drag coefficient and wake volume of single bubbles rising through quiescent liquid. *Kagaku Kogaku Ronbunshu* **2,** 480–484.

TSUCHIYA, K. & FAN, L.-S. 1986 Near-wake structure of a single gas bubble in a two-dimensional liquid–solid fluidized bed: vortex shedding and wake size variation. Presented at *AIChE A. Mtg*, Miami Beach, Fla, Paper 10b. *Chem. Engng Sci.* **43,** 1167–1181 (1988).

UNO, S. & KINTNER, R. C. 1956 Effect of wall proximity on the rate of rise of single air bubbles in a quiescent liquid. *AIChE Jl* **2,** 420–425.

WEGENER, P. P. & PARLANGE, J.-Y. 1973 Spherical-cap bubbles. *A. Rev. Fluid Mech.* **5,** 79–100.

YABE, K. & KUNII, D. 1978 Dispersion of molecules diffusing from a gas bubble into a liquid. *Int. chem. Engng* **18,** 666–671.